UNIVERSIDADE FEDERAL DE SANTA CATARINA

CAMPUS ARARANGUÁ

CENTRO DE CIÊNCIAS, TECNOLOGIAS E SAÚDE DEPARTAMENTO DE CIÊNCIAS DA SAÚDE

CURSO DE GRADUAÇÃO EM FISIOTERAPIA

JAÍNE FERRAREIS MENEGASSO

COMPÓSITO DE MONTMORILONITA-CELULOSE BACTERIANA COMO UM NOVO SISTEMA DE CURATIVO PARA LESÕES POR PRESSÃO

Araranguá

2021

JAÍNE FERRAREIS MENEGASSO

COMPÓSITO DE MONTMORILONITA-CELULOSE BACTERIANA COMO UM NOVO SISTEMA DE CURATIVO PARA LESÕES POR PRESSÃO

Artigo apresentado ao curso de Graduação em Fisioterapia, da Universidade Federal de Santa Catarina, como requisito parcial da disciplina de Trabalho de Conclusão de Curso II.

Orientador: Professor Rafael Cypriano Dutra.

Araranguá

2021

RESUMO

O principal objetivo deste estudo foi investigar os efeitos e os mecanismos de ação do hidrogel de celulose bacteriana (BC) incorporado à montmorillonita (BCH-MMT) na cicatrização de feridas cutâneas usando o modelo de lesão por pressão em camundongos. A bactéria *Komagataeibacter hansenii* foi utilizada para obter os compósitos de BC, os quais foram incorporados com MMT e caracterizados por espectroscopia de infravermelho por transformação de Fourier (FT-IR) e microscopia eletrônica de varredura (MEV). O modelo de lesão por pressão foi avaliado por análise macroscópica e histológica em camundongos *Swiss* machos. BC e BC + MMT apresentaram espectro FTIR típico de substratos celulósicos com bandas fortes em torno de 3344, 2920, 1637 e 1041 cm^{-1}, enquanto as micropartículas de MMT se dispersaram uniformemente por toda BC. Os achados desse projeto demonstram que os animais tratados com BCH-MMT apresentaram cicatrização significativa das lesões por pressão com regeneração tecidual, área reduzida de vermelhidão, inibição da hiperalgesia espontânea e células inflamatórias, bem como reepitelização completa da epiderme similarmente ao Dersani® - usado como controle positivo. Em conjunto esses resultados sugerem que o biofilme de hidrogel contendo BCH-MMT apresenta potencial como novo material curativo para lesões por pressão e ainda poderá servir como suporte para a engenharia de tecidos da pele.

Palavras-chave: celulose bacteriana; montmorilonita; regeneração de tecidos; lesão por pressão; substituto da pele.

LISTA DE ILUSTRAÇÕES

SUMÁRIO

DATA IN BRIEF TEMPLATE

***Title:**	Modified montmorillonite-bacterial cellulose composites as a novel dressing system for pressure injury
***Authors:**	Jaíne F. Menegasso[a], Nayara A. C. Moraes[a], Tatiana P. Vásquez[b], Francielly A. Felipetti[a], Regina V. Antonio[b], Rafael C. Dutra[a,c]*
***Affiliations:**	[a]Laboratory of Autoimmunity and Immunopharmacology, Department of Health Sciences, Campus Araranguá, Universidade Federal de Santa Catarina, 88906-072, Araranguá, SC, Brazil. [b]Laboratory of Biochemistry and Microbiology Applied to Biotechnological Processes, Campus Araranguá, Universidade Federal de Santa Catarina, 88906-072, Araranguá, SC, Brazil. [c]Post-Graduate Program of Neuroscience, Center of Biological Sciences, Universidade Federal de Santa Catarina, 88040-900 Florianópolis, SC, Brazil.
***Contact email:**	Rafael C. Dutra (rafaelcdutra@gmail.com)
***Co-authors**:	Jaíne F. Menegasso (jainemenegasso@hotmail.com) Nayara A. C. Moraes (naycelinca@hotmail.com) Tatiana P. Vásquez (latatiss@gmail.com) Francielly A. Felipetti (fafelipetti@gmail.com) Regina V. Antonio (regina.antonio@ufsc.br) Rafael C. Dutra (rafaelcdutra@gmail.com).
***JOURNAL:**	International Journal of Biological Macromolecules (IJBIOMAC-D-21-062700)

Title:

Modified montmorillonite-bacterial cellulose composites as a novel dressing system for pressure injury.

Authors:

Jaíne F. Menegasso[a], Nayara A. C. Moraes[a], Tatiana P. Vásquez[b], Francielly A. Felipetti[a], Regina V. Antonio[b], Rafael C. Dutra[a,c]*

Affiliations:

[a]Laboratory of Autoimmunity and Immunopharmacology, Department of Health Sciences, Campus Araranguá, Universidade Federal de Santa Catarina, 88906-072, Araranguá, SC, Brazil.

[b]Laboratory of Biochemistry and Microbiology Applied to Biotechnological Processes, Campus Araranguá, Universidade Federal de Santa Catarina, 88906-072, Araranguá, SC, Brazil.

[c]Post-Graduate Program of Neuroscience, Center of Biological Sciences, Universidade Federal de Santa Catarina, 88040-900 Florianópolis, SC, Brazil.

Contact email: Rafael C. Dutra (rafaelcdutra@gmail.com)

ABSTRACT

The main objective of this study was to investigate the effects and the underlying mechanisms of action of BC hydrogel incorporated into MMT (BCH-MMT) for skin wound healing using mice pressure injury model. *Komagataeibacter hansenii* was used to obtain the BC composites, which were incorporated with MMT and characterized through Fourier transform infrared spectroscopy (FT-IR), and Scanning Electron Microscopy (SEM). Pressure injury model was assessed by macroscopic and histological analysis in male Swiss mice. BC and BC+MMT showed a typical FTIR spectrum of cellulosic substrates with strong bands at around 3344, 2920, 1637, and 1041 cm^{-1}, and microparticles of MMT showed disperse uniformly throughout BC. To our knowledge, our findings showed for the first time that animals treated with modified BCH-MMT showed significant healing of pressure ulcers with tissue regeneration, reduced area of redness, spontaneous hyperalgesia, complete re-epithelialization of the epidermis and inhibited inflammatory cells similarly to Dersani® used as a positive control. Altogether, these findings suggest that a modified BCH-MMT hydrogel film have the potential to be a novel dressing material for pressure injury and a scaffold for skin tissue engineering.

Keywords: bacterial cellulose; montmorillonite; tissue regeneration; pressure injury; skin substitute.

1. INTRODUCTION

The skin is the largest organ of the body and, when intact, has important physiological functions such as thermoregulation, blood reservoir, sensitivity, excretion and absorption of substances, and synthesis of vitamin D. Moreover, the skin also functions as a powerful barrier against external mechanical aggressors and prevents pathogens from entering the body [1, 2]. However, the discontinuity of the cutaneous tissue favors microbial contamination, especially in wounds that are difficult to heal, such as pressure injuries [3].

Pressure injury is a skin injury resulting from the compression between bony prominences and the patient's external surface. This condition results in necrosis and reduced quality of life, especially in elderly individuals with restricted mobility [4]. Ischemia and reperfusion cycles are the main causes of pressure injuries. However, the lack of mobility, lack of local humidity, diabetes mellitus, and smoking can potentiate the lesion and form ulcers, impairing the healing of these wounds [5]. The worldwide epidemiological data described by Zhaoyu and colleagues demonstrated that the prevalence of pressure injuries is 12.8% [6]. Consequently, pressure injury represents a significant financial burden for healthcare organizations [7-9]. Thus, the design and execution of adequate protocols for the prevention of pressure injuries can help prevent the evolution of these injuries. However, Barker and authors have stated that prevention strategies do not achieve a significant reduction in the prevalence of pressure injuries [10]. For this reason, some researchers argue that more specific, selective, and less toxic therapies are needed to treat pressure ulcers [11, 12]. The active components derived from non-pathogenic microorganisms have been widely used as therapy for some cutaneous lesions and have alternated the history of many types of skin diseases [11, 12].

The bacterial cellulose membrane (BC) is a natural biopolymer synthesized by different strains of bacteria, such as *Acetobacter*, *Achromobacter*, *Aerobacter*, *Agrobacterium*, *Alcaligenes*, *Azotobacter*, *Escherichia*, and *Komagataeibacter* [13]. BC has important biological properties such as biocompatibility and non-toxicity as well as essential mechanical properties, including moisture retention. In this way, BC is a suitable candidate for biomedical and biotechnological applications and can help in the healing of skin lesions [2]. However, BC has limited antimicrobial activity, and for this reason, BC has been used as a matrix for the production of nanocomposites, aiming to integrate new properties [14]. Montmorillonite (MMT), also called smectite

($Mx(Al_4\text{-}xMg_x)Si_8O_{20}(OH)_4$), is the main component of clay. Previous studies have demonstrated that MMT has important therapeutic activity and can be applied in the medical field for skin cleaning and protection. Moreover, MMT can repair tissue, activate blood clotting and has demonstrated antibacterial properties, as it is able to adsorb bacteria such as *Escherichia coli* and *Staphylococcus aureus* and neutralize toxins [15, 16]. MMT hydrogel is a transparent compound, consisting of approximately 77.7% water, 2.3% carboxymethylcellulose, and 20% propylene glycol. Previous studies have demonstrated that hydrogels have therapeutic efficacy in removing crusts from devitalized tissue, present in open wounds, through autolytic debridement. Furthermore, hydrogels also moisturize cutaneous lesions, thus favoring debridement and, subsequently, healing [1, 17-19]. Keeping the above data in mind, the main objective of this study was to investigate the potential of the bacterial cellulose hydrogel incorporated into montmorillonite (BCH-MMT) for tissue healing and repair using the pressure injury model in mice.

2. MATERIALS AND METHODS

2.1. Materials

Montmorillonite cloisite 20A (Cloisite®) was acquired from Buntech Tecnologia de Insumos (São Paulo, SP, Brazil). Glucose, peptone and yeast extract were purchased from Acumedia® (Neogen Culture Media, Lansing, MI, USA). Anhydrous sodium bicarbonate, citric acid monohydrate and sodium hydroxide were obtained from Neon® (Suzano, SP, Brazil). Hydroxyethylcellulose (Cellosize® QP-4400H Hydroxyethyl Cellulose) from Dow® (Dow Way Midland, MI, USA). Propylene glycol (Kollisolv® PG) from BASF (São Paulo, SP, Brazil). Methyl 4-hydroxybenzoate (Nipagin®), paraffin, and Mallory's trichrome from Sigma-Aldrich (St. Louis, MO, USA). Formaldehyde was obtained from Merck (Frankfurt, Darmstadt, Germany). Hematoxylin and eosin were purchased from Solarbio Science & Technology (Beijing, China). Neodymium magnets from Magnetic Source (Castle Rock, CO, USA). Dersani® (hydrogel with alginate) was obtained from Laboratório Daudt Oliveira LTDA (Rio de Janeiro, RJ, Brazil). Paracetamol plus codeine phosphate was purchased from EMS Laboratory (São Bernardo do Campo, SP, Brazil). Ketamine hydrochloride and xylazine hydrochloride were obtained from Agener União® and Dopaser®, all from Brazil, respectively. Ethanol was obtained from Dinâmica Química Contemporânea

(Indaiatuba, SP, Brazil). Potassium bromide p.a. (KBr) was purchased from Vetec Química Fina (Duque de Caxias, RJ, Brazil). The other reagents used were of analytical grade and obtained from different commercial sources.

2.2. Synthesis of bacterial cellulose membrane (BC) and montmorillonite (BC+MMT) incorporation

Komagataeibacter hansenii (ATCC line 23769) and Hastrin & Schramm culture medium were used to obtain the BC [20, 21]. BC was produced according to the following steps: culture, lyophilization, spraying, and rehydration. The culture medium had the following composition glucose (20 g/L), peptone (5 g/L), yeast extract (5 g/L), anhydrous sodium bicarbonate (2.7 g/L), and citric acid monohydrate (1.15 g/L). Then, for BC purification, a solution of 0.1 M NaOH was used at 90°C for 20 minutes to remove bacterial impurities and culture residues [21, 22]. After this procedure, the BC was washed with running water, then washed with sterile distilled water, and finally stored in 20% ethanol solution at 10°C. After 24 hours, BC sheets circular in shape, measuring 5 cm in diameter, were submerged in a suspension of MMT at 0.1% and were stirred at 100 rpm for 24 hours at 28°C. After that, BC sheets incorporated with MMT were removed from the suspension and stored at 10°C, for the further preparation of BCH+MMT [2, 21].

2.3. Synthesis of hydrogel (BCH-MMT)

Initially, BC+MMT was solubilized in distilled water under magnetic stirring at room temperature – high-speed dispersing element (Ultra-Turrax®, model T25, Germany). After complete homogenization, a suspension of BC+MMT particles was obtained and sifted in a 37-mesh sieve to remove water, leaving only a paste with BC+MMT microparticles. Next, hydrogel formulation (BCH-MMT) was prepared by mixing the reagents. For the formulation of 100 g of BCH-MMT the following reagents were used: 4.5 g hydroxyethylcellulose, 7.5 g propylene glycol, and 0.30 g methyl 4-hydroxybenzoate [23, 24]. Briefly, methyl 4-hydroxybenzoate was solubilized in hot propylene glycol under manual stirring. Subsequently, these reagents were poured into a beaker containing 12 g of bacterial cellulose. Thereafter, the hydroxyethylcellulose was slowly added to obtain the gel consistency of the gel. Finally, 75.7 g of distilled water was added, finalizing the hydrogel (BCH-MMT) [23].

2.4. Chemical and morphological evaluation of BC and BC+MMT

BC and BC+MMT chemical evaluations were performed by Fourier transform infrared spectroscopy (FT-IR). First, BC and BC+MMT were ground to a powder, pressed into KBr pellets, and finally analyzed. FT-IR was recorded on Agilent Technologies Cary 600 Series spectrometer with a spectral range from 500 to 4,000 cm^{-1}. BC and BC+MM morphological evaluations were performed by scanning electron microscopy (SEM). BC and BC+MMT were dehydrated with an increasing ethanol series (20%, 50%, 70%, and 100%), dried, and metalized with gold in a critical-point chamber using carbon dioxide as the exchange agent [25]. The electron microscopy work was performed on a JEM-1011 microscope at Central Laboratory of Electronic Microscopy-UFSC, Florianópolis, Brazil.

2.5. Mechanical properties of BC and BC+MMT

The tensile evaluation was performed on TA.HDplus Texture Analyser machine (Stable Micro Systems) at room temperature, at a 1 mm/minute speed with a 1000 N sensor loaded. The mean value was obtained from at least five strip samples with a 1 x 5 cm size, and the thickness of 5 random points on the strip was measured with a micrometer.

2.6. Animals

The experiments were performed in male Swiss mice (30-40 g), 10-12 weeks old, obtained from the Universidade Federal de Santa Catarina, and experiments were performed in the Laboratory of Autoimmunity and Immunopharmacology. The mice were housed in individual cages under standard conditions of temperature and light (12:12 h light/dark cycle, lights on at 07:00) and were given free access to food and water. All procedures used in the present study were approved by the Animal Ethics Committee of the Federal University of Santa Catarina (CEUA-UFSC, protocol number 4816200917), and were performed in accordance with the “Principles of Laboratory Animal Care” from NIH publication No. 85-23. The number of animals and the intensity of noxious stimuli used were the minimum necessary to demonstrate consistent effects. All of the experimental procedures were conducted according to the guidelines of CONCEA and CEUA/UFSC, based on the principles of the 3Rs (Replacement, Reduction, and Refinement).

2.7. The experimental model of pressure injury

For pressure injury induction, animals were randomly divided into the following groups: i) control group (n = 9), pressure injury without treatment; ii) BCH-MMT group (n = 9), pressure injury treated daily with 0.25 g BCH-MMT; iii) Dersani group (n = 10), pressure injury treated daily with 0.25 g Dersani®. After dividing the groups, the animals were intraperitoneally anesthetized with 10 µl ketamine hydrochloride (90 mg/kg) associated with xylazine hydrochloride (10 mg/kg). The animals were placed on a properly cleaned surgical bench to perform the trichotomy and asepsis (70% alcohol) of the dorsal region [26, 27]. On the subsequent days, two neodymium magnets (dimensions: 12 mm in diameter and 0.5 mm in thickness) were used to induce the pressure injury. The experimenters formed a fold in the skin of the animals' back and placed two magnets, thus exerting compression of the skin positioned between the magnets. A magnetic force of 1800 Gauss was used, totaling an average force of 3600 Gauss. Four cycles of ischemia-reperfusion were necessary. Each cycle consisted of 12 hours with the magnets, followed by 12 hours without the magnets (ischemia-reperfusion), resulting in two injuries *per* animal [28]. After the installation of the pressure lesion, the animals received a combination of paracetamol (200 mg/kg) and codeine phosphate (30 mg/kg), which were administered in water available in the drinking fountain during three consecutive days. Finally, the animals were evaluated for 15 days to check the healing of the wounds [29, 30].

2.8. Macroscopic evaluation and hyperalgesia behavior

Pressure injuries were assessed macroscopically to investigate the effect of BCH-MMT. On days 0, 3, 5, 7, 10, 12, and 15 after induction, the length and width of each wound were measured using a universal analog steel manual caliper (Mitutoyo, series 530, capacity 200 mm/8", 0.02 mm/0.01", Japan), positioned at the edges of the lesions. The wound size was calculated based on the area of an ellipse: length radius × width radius × π. In addition to the lesion contraction parameters, the presence of exudate, redness and wound moisture was also observed, using the following scores: +: absent; ++: moderate, and +++: intense [30]. Finally, the evaluation of the hyperalgesia score using the animals' facial expressions was performed, according to the grimace scale [31]. All behavioral data were measured manually, and the observer was totally blind to the experimental protocol for all tests.

2.9. Histological analysis

On days 5, 10, and 15 animals were euthanized, and the tegument tissue was collected, fixed in 4% paraformaldehyde solution, and subjected to conventional histological processing [32]. First, the tissue was cut in halves and divided into anterior and posterior fragments. Only the posterior fragment was used for this analysis and, therefore, it was dehydrated, diaphanized, and embedded in paraffin to obtain blocks [32]. The blocks were then adapted in a semi-automatic microtome to obtain sections of 6 µm thickness. As a standard, 18 consecutive sections of tissue blocks were collected, and six histological slides were prepared. The slides were stained using Mallory's trichrome or hematoxylin and eosin (H&E). Then, the slides were photographed using the Top View program and a camera attached to a light microscope. The images were recorded at 400x magnification and analyzed using the Image J program by a single examiner. The wound healing process and the presence of collagen were demonstrated using descriptive analysis. The number of inflammatory cells at the borders of the lesion was examined by histomorphometric analysis. The quantified values were compared between the groups.

2.10. Statistical analysis

Data were analyzed using GraphPad Prism software version 8.2.1 for Windows (San Diego, CA, USA). The one-way and two-way analysis of variance (ANOVA) was performed to analyze the differences among experimental groups, and $p < 0.05$ was defined as statistically significant. Results are expressed as the mean ± standard error of the mean (SEM).

3. RESULTS

3.1. Chemical, morphological and mechanical evaluation of BC and BC+MMT

The FT-IR analysis for BC and BC+MMT is shown in Fig. 1. All the corresponding bands of BC in the fingerprint region can be seen in the spectrum of BC+MMT. BC and BC+MMT showed a typical FTIR spectrum of cellulosic substrates with strong bands at around 3344, 2920, 1637, and 1041 cm^{-1}. These bands are associated, respectively, with the vibrations of the OH, CH, C = O, and C-O-C groups of cellulose [33, 34]. Bands at around 1425-1100 showed evidence of contamination with residual proteins. After MMT incorporation, BC+MMT presented bands at around 3344, 1637,

1062, and 646 cm^{-1}. The increase in the band around 3344 is related to the OH stretching of the constituent of the octahedral sheet and adsorbed water on the MMT surface. At 1637 cm^{-1}, the band raise refers to OH bending vibration of adsorbed H_2O [2]. The one at 1062 cm^{-1} is related to Si-O stretches. The bending vibration peaks for Mg single bond O appeared at ~886 cm^{-1} [22]. Deformation vibrations at 646 cm^{-1} refer to Si-O-Al [35]. Taken together, the FT-IR spectra give convincing clues of the formation of the BC+MMT composites. Additionally, Fig. 2 shows a possible interaction between BC and MMT particles based on both structures and FTIR results. MMT is composed of two tetrahedral silica layers sandwiching an octahedral alumina layer. The silica layers are inward-pointing toward the octahedral layer. It has an interlayer gallery with exchangeable cations where inter-chain hydrogen bonds between the hydroxyl groups of cellulose chains can be attached. The SEM micrographs of BC presented the typical homogeneous surface of bacterial cellulose (Fig. 3A). Results of SEM on Fig 3B showed that BC was successfully modified with MMT adhered on BC surface. The tridimensional network of nano and microfibrils of cellulose in the approximate range of 10-70 nm could be observed in Fig. 3C. Microparticles of MMT presented disperse uniformly throughout BC (Fig. 3D). MMT was much bigger than the diameter of nano and microfibrils of cellulose and tightly and uniformly attached at microfibers' surface. Finally, Fig. 3E and F showed a macrostructure of BC membranes without MMT and MMT, respectively. Interestingly, it was observed that MMT particles turned the BC membrane-less translucent and with a whiter coloration, typical of MMT.

Mechanical properties are important parameters for estimating the quality and biomedical applications of BC composites. Herein, our results indicated that the maximum tensile strength at the breaking point for BC+MMT was higher than for pure BC (Fig. 4). Similar increases in the polymer's tensile properties–clay composites have also previously been reported [22, 36]. The tensile strength for pure BC was found to be 30 MPa, which increased to 38.5 MPa. It is known that MMT particles get attached to the BC network through hydrogen bonding and Van der Waals interactions [37, 38], which strengthens the fibrils and enhances the overall toughness of the BC. Moreover, the MMT particles incorporated into the BC sheets restrict the polymer chains' mobility and thus increase the toughness and mechanical strength of the composites [36, 39]. Similarly, Young’s modulus for BC+MMT was 7.08 ± 2.2 MPa, slightly higher than pure BC (6.7 ± 3.1). The elasticity of the composite materials decreased with clay

incorporation shown in Fig. 4 because these can result in fractures of the composite surface. Thus, the breaking point is attained at a lower strain for BC+MMT. The strain on the breaking point was at ~16%, while pure BC was ~17% (Fig. 4). The results showed that the mechanical properties of BC-MMT hydrogels were improved compared to those of pure BC by incorporating MMT particles. Taken together, this could be an important driving factor for the industrial and biomedical applications of BC–MMT composites.

3.2. Macroscopic and hyperalgesia analysis

Healing is a dynamic and complex sequence of several events that begin shortly after an injury to restore tissue integrity [2]. In this study, the parameters used for the assessment of macroscopic healing were analysis of the wound area, percentage of contraction of the lesion, exudate, redness, moisture, and spontaneous hyperalgesia. The periodic evaluation of these parameters showed pattern of healing of the lesion. The wound area analysis is shown in Fig. 5A and 5B. Starting day 3, the group treated with BCH-MMT showed wound reduction when compared to the control group. The effect of BCH-MMT started right at the injury induction stage, thus preventing its progression and development. Moreover, this effect accelerated the process of complete healing, similarly to Dersani®, a medication clinically used to treat pressure injuries. Relevantly, treatment with BCH-MMT showed a statistically significant difference on days 3, 5, and 7 when compared to the control group (Fig. 5B). The exudate analysis is shown in Fig. 5C and no significant differences are observed between groups. The redness analysis is shown in Fig. 5D. Starting day 3, the BCH-MMT treatment significantly inhibited the redness of the lesion when compared to the control group. This effect was even better than the effect of Dersani®, which reduced redness only on day 7. The effect of BCH-MMT on redness characterized the effectiveness of this product in reducing one of the five cardinal signs of inflammation. The moisture analysis is shown in Fig. 5E. On days 3, 5, and 7, the BCH-MMT group showed similar moisture to that observed in the baseline period. This effect showed that BCH-MMT could maintain adequate moisture from pressure injuries, which favors healing, similarly to Dersani®, used as a positive control. The spontaneous hyperalgesia analysis is shown in Fig. 5F. The group treated with BCH-MMT showed a reduction in spontaneous hyperalgesia, markedly in the first days after the injury was induced, similarly to Dersani®, used as a positive control. Importantly, BCH-MMT

treatment markedly inhibited hyperalgesia behavior on day 3 when compared to the control group.

3.3. Microscopic analysis

The conventional histological technique using light microscopy is widely employed to assess wound healing and regeneration progress at the tissue level [2]. In the present study, microphotographs of H&E and Mallory's trichrome stained sections showed an interesting pattern of wound regeneration. These results are shown in Fig. 6, 7, and 8. After 5 days of treatment, the BCH-MMT treated group showed a normal wound healing cascade, with an area of congestive blood vessels (hyperemia), fluid accumulation (edema), fibroblasts (Fig. 6), and fine collagen fibers deposition beneath the wound (Fig. 7). Furthermore, an intense inflammatory infiltrate was observed (Fig. 8). On day 10, part of the wound re-epithelialized, and a granulation tissue plus proliferation of blood vessels were noticed below the wound, filling the tissue area that was destroyed (Fig. 7). After 15 days of treatment, the BCH-MMT treated group showed a decrease in the number of inflammatory cells (Fig. 8). Moreover, the wound surface of the BCH-MMT group was covered with healthy regenerated epithelial cells, without ulcerations, and achieved complete re-epithelialization, similarly to the Dersani® group (Fig. 6). Furthermore, reabsorption of the granulation tissue, reduction of blood vessel numbers, reduction of edema, more aligned fibroblasts (Fig. 6), and more resistant collagen fibers (Fig. 7) were observed. On the other hand, in this period, the control group showed greater inflammatory cells, the presence of necrotic tissue, and ulceration, which indicates that the wound healing process progressed only to the inflammatory stage, without re-epithelialization (Fig. 6 and 8). In brief, the present results showed improvement in wound healing and tissue regeneration in BCH-MMT treated groups in comparison to the control group. This improvement effect accelerated the process of complete healing, similarly to Dersani®, a medication used clinically to treat pressure injuries.

4. DISCUSSION

Pressure ulcers have a significant impact on patients' lives, health care, and society. Despite the increase in preventive care, the prevalence of pressure ulcers has remained virtually unchanged, while the associated costs and care continue to be lower. Therefore, the development of new prevention and treatment strategies are

necessary to complement the quality of care and reduce the financial burden imposed on health services [6-8]. Evidence refers to the need to improve the understanding of the pathophysiology of these lesions to develop new techniques and therapeutic approaches to wound care [10].

Over the last decade, promising results have been reported and applied to bacterial cellulose membranes (BC) as a wound healing biomaterial [40]. Previous studies showed that hydrogels from BC have hydrophilic properties and efficacy in maintaining the appropriate water balance [12, 41]. However, BC failed to inhibit bacteria during infections [2]. On the other hand, MMT has demonstrated antibacterial properties [15, 16] and the ability to activate blood coagulation factor XII, leading to the triggering of the intrinsic blood coagulation pathway [42]. Given this information, it can be suggested that the incorporation of MMT into BC improves the properties of BC for biomedical applications [21]. Herein, in this work, BC was incorporated with MMT to produce a hydrogel, and to further investigate the effect of this product on the healing of pressure lesions in mice.

In this study, BCH-MMT showed a complex structure, with adsorbed water molecules. According to Portela and colleagues, BC fibers are composed of glucan chains linked through inter and intramolecular hydrogen bonds. This feature allows BC to be elastic and mechanically robust [21]. The absorbed water molecules are responsible for maintaining the crucial level of BC hydration, a fundamental characteristic of this compound for medical applications. BCH-MMT maintained adequate moisture in pressure injuries. Other studies have confirmed and extended these previous data, which demonstrated that BC promotes healing, keeps the wound moist, and controls wound exudates [43, 44]. Some of the main characteristics necessary for healing injuries are the water content and water retention properties, to keep the wound hydrated, and to absorb large amounts of exudates [21]. The presence of exudates causes the separation of tissue layers from the wound, which slows down the healing process. Therefore, exudates must be eliminated from the wound and good drainage capacity is recommended [21]. Drainage capacity and adequate control of moisture generally increase healing rates and protect the wound from infections [45]. The ability to maintain moisture also prevents the dressing from dehydrating and prevents it from attaching to the wound, and reducing pain during dressing changes [46]. As a moist environment encourages rapid healing, hydrogels are ideal candidates for the development of dressings [45, 47]. Therefore, BCH-MMT

may have maintained adequate moisture from pressure injuries due to the abovementioned properties.

Additionally, BCH-MMT treatment decreased ulcer size, contracted the lesion, and reduced redness in pressure lesions in treated mice. The results demonstrate the best capacity of BCH-MMT dressings for faster wound healing compared to the control group. Interestingly, our data corroborate those found by Sajjad and colleagues [2]. Nonetheless, we do not intend to directly compare or dispute results since most discrepancies reside on the differences between experimental models, and the methodology applied is mostly different. A pressure injury used in this study is defined as a skin lesion resulting from compression between bony prominences and the patients' external surface, which induces necrosis, pain, and reduced quality of life, mainly in aging individuals. Herein, we used a pressure ulcers model, in which two neodymium magnets were compressed in the skin, inducing microvascular occlusion and soft tissue blood supply depletion. Consequently, oxygenation is restricted, resulting in tissue ischemia and hypoxia. Ischemia followed by hypoxia induces a pro-inflammatory environment. During reperfusion, excessive leukocytes and neutrophils migrate to the wound and produce inflammatory cytokines and reactive oxygen and nitrogen species (RONS). The repetition of periods of ischemia followed by reperfusion can lead to deleterious effects on the tissue, causing necrosis and tissue ulceration in the region affected by pressure. Therefore, the pressure injury is a wound that occurs from the inside out, as previously described [48]. In the present work, once the ulcer inflicted the skin, we applied the BCH-MMT. Additionally, the composites' application was facilitated by the production of the hydrogel, which was daily applied on the lesion. On the other hand, Sajjad et al. (2019) used a completely different experimental model induced by a burn, in which a designed metal bar heated on flame was applied to the skin [2]. Importantly, burned model and burned injury occurs from outside to inside. Burn follows after the skin is damaged by heat, electricity, chemicals, or radiation. After damage, the skin's integrity is lost, and it becomes susceptible to fluid loss, electrolyte dysregulation, and infection by pathogens. Moreover, the release of pro-inflammatory mediators, such as tumor necrosis factor (TNF) and interleukins (IL-6, IL-8, and IL-1β), can lead to systemic repercussions, depending on the degree and extent of the burn through nuclear factor κB (NF-κB) pathway inducing biphasic response. The first phase is systemic inflammatory response syndrome, and the major immune cell is M1 type macrophages, which release cytokines and inflammatory mediators involved with

the innate immune response. Furthermore, burn injury triggers significant apoptosis of organ cells by proapoptotic factors, like caspase-3, Bcl-xl, and Bax proteins. Importantly, bradykinin (BK), a powerful vasoactive mediator, is produced at the burn injury site and induces vascular dilation, upregulation of microvascular permeability, smooth muscle contraction, and pain. The second phase is a pro-resolution syndrome, which depends on M2 type macrophages and T lymphocytes of helper Th-2 associated to three principal mediators: IL-4/IL-10 and TGF-β [49, 50]. Additionally, Sajjad and colleagues used another Gram-negative aerobic bacteria (*Gluconacetobacter xylinus*) to obtain a BC membrane incorporated with MMT to investigate this product's effect in wound healing activities. Another difference between Sajjad and our study resides in the fact that after burn induction, they applied 3 x 3 cm BC-MMT membrane on the lesion and fixed it with a disposable skin stapler. Their wound healing experiment continued for 15 days, and the membranes were changed on days 5 and 10. Taken together, these researchers found that the membrane decreased ulcer size, contracted the lesions, and enabled a good healing pattern without signs of lesion infection [2]. Despite the great progress observed in the preceding decades using cellular and pharmacological techniques regarding the mechanisms that underlie the control of pressure injury, few effective and safe biotechnological and immunomodulatory therapies have emerged. According to Shpichka and colleagues, skin wound healing is a serious interaction between cell types, cytokines, mediators, the neurovascular system, matrix remodeling, and tissue regeneration technology that remarkably enhances skin repair re-epidermalization, epidermal-stromal cell interactions, angiogenesis, and inhabitation of hypertrophic scars and keloids [50]. Although Sajjad and co-authors made the similar analysis demonstrated in the present work, we highlight that there were differences in the methodology applied, such as i) way in which the product was applied, ii) the frequency of changing the dressing, iii) the preclinical model used, and last but not least, iv) the pathophysiology of the studied disease. Therefore, we emphasize that the results describe by Sajjad et al. (2019) cannot be extrapolated to the results of the present work – in turn, and it is impossible to compare our results with Sajjad data directly. Moreover, the previous manuscript does not compromise the novelty of our data. However, instead, it reinforces our initial proposal about the relevance of modified montmorillonite-bacterial cellulose composites as a novel dressing system for pressure or burns injuries, since the accumulation of evidence enables scientific

progress on the subject, promotes the deepening of knowledge of the facts and the improvement of investigation methods. Relevantly, this epistemological consensus is fundamental to the scientific paradigm, as it establishes agreement and legitimacy around important issues for society and is responsible for advancing scientific responses to problems. In this context, Kuhn (2012) challenge long-standing linear notions of scientific progress, arguing that transformative ideas do not arise from the day-to-day, gradual process of experimentation and data accumulation but that the revolutions in science, those breakthrough moments that disrupt accepted thinking and offer unanticipated ideas, occur outside of “normal, neutral, conventional and obvious science” [51-53].

Another study conducted by Xu and colleagues found that the application of cellulose hydrogel also decreased lesion size [54]. These results agree with other studies that used hydrogel nanocomposite dressings and observed that the wound surface of the treated group was reduced when compared to the control group [42]. Interestingly, the deposition of the hydrogel forms a thin layer with small fibers of cellulose, serving as a barrier against external agents and favoring healing [55]. Taken together, these findings can be attributed to the creation of a moist environment on the wound surface in the presence of the dressing. This fact favors the migration of epidermal cells, which is faster on a moist surface compared to the conditions that exist under a scab on a dry wound [42].

Added to the data discussed above, the present study also demonstrated that, after 15 days, the BCH-MMT treated group had completely healed wounds, with extensive epithelial re-epithelialization. These findings corroborate the studies of Loh and authors, who also observed re-epithelialization and complete healing in their hydrogel-treated mice [55]. In a study conducted by Kawak and colleagues, where burned skin tissues of rats were treated with BC, marked dermal and epidermal healing were observed [56]. Even, Sajjad and colleagues observed that the lesions contracted more quickly in the treated groups compared to the control [2]. After injury, the healing process involves a sequence of several events to restore tissue integrity. First, blood clotting occurs, with stimulation of the immune system, called cell homeostasis. After that, inflammatory cells, such as neutrophils, lymphocytes, monocytes, and macrophages migrate into the wound to initiate tissue repair, i.e. the typical inflammatory phase. Then cell proliferation occurs (fibroblasts), as well as angiogenesis and re-epithelialization (mainly via keratinocyte proliferation). In the

latter stage, called the remodeling phase, increasing resistance of the damaged tissue shows characteristics close to those of the original tissue [57, 58]. Sirousazar and colleagues stated that hydrogels may favor the first phase of the healing process because of the negative charge on its surface, which activates blood clotting factors. Furthermore, complete healing can be attributed to the presence of growth factors, fibroblast activity, increased deposition of fibrinogen and fibronectin, and accelerated debridement. All of these factors may have contributed to the easier and faster migration of epidermal cells under the dressings [42]. Herein, we speculate that BCH-MMT may stimulate an increase in tissue regeneration factors and reach the remodeling phase quicker after pressure injury, similar to the Dersani® group, although further in vivo and molecular experiments are needed to confirm this hypothesis. These results indicate that the BC derivatives incorporated into MMT exhibit an important therapeutic potential for the treatment of skin lesions [2].

After 15 days, the BCH-MMT treated group showed a significant decrease in the number of inflammatory cells, similar to the Dersani® group. These findings corroborate the studies of Loh and colleagues who also observed a reduction in the number of inflammatory cells in the mice treated with a pure hydrogel biomaterial [55]. Kawak and colleagues showed that BC treatment inhibited mast cell proliferation from day 5 to day 15 in a skin burn model [56]. All these results are in accordance with the findings of Brassolati, who propose that the satisfactory evolution of the healing process and inflammation is due to a decrease in the inflammatory infiltrate [59].

Finally, a reduction in spontaneous hyperalgesia was observed in the group treated with BCH-MMT when compared to the control group, through the evaluation of the grimace scale. According to Langford and colleagues, the grimace scale is used to analyze the degree of hyperalgesia of animals through facial expressions [31]. Importantly, we have not found any studies in the literature that verify this parameter in a preclinical cutaneous lesions model. Thus, we suggest that the reduction of the spontaneous hyperalgesia level observed in the BCH-MMT treated animals was due to the control of inflammatory manifestations. Bourakadi and colleagues found that MMT showed effective antibacterial action, as it absorbs bacteria from the microenvironment and immobilizes them on its surface [60]. Moreover, MMT also promotes hygiene, skin protection, healing, and blood clotting [61]. Therefore, it is possible to suggest that all these factors contributed to the control of the inflammatory process and infection, resulting in a decrease in hyperalgesia as evidenced by the

grimace scale. Relevantly, the characteristics described for BCH-MMT, together with biocompatibility, non-toxicity, and a favorable cost-benefit ratio, demonstrate the fundamental properties for dressing applications.

The limitation of our study was the lack of antimicrobial property of the composite, which could reinforce the advantages of BC-MMT hydrogel as a dressing material compared with native BC hydrogel. In fact, we carried out a pilot protocol to investigate the antimicrobial potential of the composites using *Escherichia coli* DH10B. However, the results were inconclusive, thus justifying future experiments and new repetitions. Additionally, due to the current coronavirus COVID-19 pandemic – a global health crisis – that affected the routine of the university, further investigations are permanently suspended, making it unfeasible to conduct additional experiments.

5. CONCLUSIONS

In summary, the BCH-MMT used in the present study represents a novel compound for the treatment of pressure injuries. This biotechnological product induced cutaneous healing of pressure lesions in mice with a significant reduction in the lesion area, reduced inflammatory signs such as redness and hyperalgesia, and the maintenance of adequate humidity. Moreover, BCH-MMT treatment completely re-epithelialized the wound 15 days after reperfusion. Taken together, this study suggests that modified BCH-MMT hydrogel films could be a novel dressing material for pressure injury and a scaffold for skin tissue engineering.

CRediT authorship contribution statement

Jaíne F. Menegasso: Methodology, Software, Data curation, Writing - original draft, Visualization, Investigation, Writing - review & editing. **Nayara A. C. Moraes**: Methodology, Software, Data curation, Visualization, Investigation, Writing - review & editing. **Tatiana P. Vásquez**: Methodology, Software, Data curation, Writing - original draft, Visualization, Investigation, Writing - review & editing. **Francielly A. Felipetti**: Methodology, Software, Data curation, Writing - original draft, Visualization, Investigation, Writing - review & editing. **Regina V. Antonio**: Methodology, Software, Data curation, Writing - original draft, Visualization, Investigation, Writing - review & editing. **Rafael C. Dutra**: Methodology, Data curation, Writing - original draft, Visualization, Investigation, Writing - review & editing, Conceptualization, Funding acquisition, Supervision.

Declaration of competing interest

The authors declare that they have no known competing financial interests or personal relationships that could have appeared to influence the work reported in this paper.

Acknowledgments

We thank Roger Flores Ceccon for scientific and philosophical support. This work was supported by Conselho Nacional de Desenvolvimento Científico e Tecnológico (CNPq), Coordenação de Aperfeiçoamento de Pessoal de Nível Superior (CAPES), Fundação de Apoio a Pesquisa e a Inovação do Estado de Santa Catarina (FAPESC), INCT-INOVAMED Program (Grant 465430/2014-7), Programa de Pós-Graduação em Neurociências (PGN), Laboratório Multiusuário de Estudos em Biologia (LAMEB), and Laboratório Central de Microscopia Eletrônica (LCME), all from Brazil. JFM is an undergraduate student in physiotherapy and has received a grant from CNPq. RCD is the recipient of a research productivity fellowship from CNPq.

REFERENCES

[1] A.A. Chaudhari, K. Vig, D.R. Baganizi, R. Sahu, S. Dixit, V. Dennis, S.R. Singh, S.R. Pillai, Future Prospects for Scaffolding Methods and Biomaterials in Skin Tissue Engineering: A Review, International journal of molecular sciences 17(12) (2016).

[2] W. Sajjad, T. Khan, M. Ul-Islam, R. Khan, Z. Hussain, A. Khalid, F. Wahid, Development of modified montmorillonite-bacterial cellulose nanocomposites as a novel substitute for burn skin and tissue regeneration, Carbohydrate polymers 206 (2019) 548-556.

[3] A. Stejskalova, B.D. Almquist, Using biomaterials to rewire the process of wound repair, Biomaterials science 5(8) (2017) 1421-1434.

[4] L.E. Edsberg, J.M. Black, M. Goldberg, L. McNichol, L. Moore, M. Sieggreen, Revised National Pressure Ulcer Advisory Panel Pressure Injury Staging System: Revised Pressure Injury Staging System, Journal of wound, ostomy, and continence nursing : official publication of The Wound, Ostomy and Continence Nurses Society 43(6) (2016) 585-597.

[5] F. Coyer, S. Miles, S. Gosley, P. Fulbrook, K. Sketcher-Baker, J.L. Cook, J. Whitmore, Pressure injury prevalence in intensive care versus non-intensive care patients: A state-wide comparison, Australian critical care : official journal of the Confederation of Australian Critical Care Nurses 30(5) (2017) 244-250.

[6] Z. Li, F. Lin, L. Thalib, W. Chaboyer, Global prevalence and incidence of pressure injuries in hospitalised adult patients: A systematic review and meta-analysis, International journal of nursing studies 105 (2020) 103546.
[7] Z. Moore, US Medicare data show incidence of hospital-acquired pressure ulcers is 4.5%, and they are associated with longer hospital stay and higher risk of death, Evidence-based nursing 16(4) (2013) 118-9.
[8] C. Dealey, J. Posnett, A. Walker, The cost of pressure ulcers in the United Kingdom, Journal of wound care 21(6) (2012) 261-2, 264, 266.
[9] R.S. Kirsner, G. Delhougne, R.J. Searle, A Cost-Effectiveness Analysis Comparing Single-use and Traditional Negative Pressure Wound Therapy to Treat Chronic Venous and Diabetic Foot Ulcers, Wound management & prevention 66(3) (2020) 30-36.
[10] A.L. Barker, J. Kamar, T.J. Tyndall, L. White, A. Hutchinson, N. Klopfer, C. Weller, Implementation of pressure ulcer prevention best practice recommendations in acute care: an observational study, International wound journal 10(3) (2013) 313-20.
[11] G.F. Picheth, C.L. Pirich, M.R. Sierakowski, M.A. Woehl, C.N. Sakakibara, C.F. de Souza, A.A. Martin, R. da Silva, R.A. de Freitas, Bacterial cellulose in biomedical applications: A review, International journal of biological macromolecules 104(Pt A) (2017) 97-106.
[12] J.M. Rajwade, K.M. Paknikar, J.V. Kumbhar, Applications of bacterial cellulose and its composites in biomedicine, Applied microbiology and biotechnology 99(6) (2015) 2491-511.
[13] Y. Yamada, P. Yukphan, H.T. Lan Vu, Y. Muramatsu, D. Ochaikul, S. Tanasupawat, Y. Nakagawa, Description of Komagataeibacter gen. nov., with proposals of new combinations (Acetobacteraceae), The Journal of general and applied microbiology 58(5) (2012) 397-404.
[14] H.S. Barud, T. Regiani, R.F.C. Marques, W.R. Lustri, Y. Messaddeq, S.J.L. Ribeiro, Antimicrobial bacterial cellulose-silver nanoparticles composite membranes, J Nanomater 2011(ID 721631) (2011) 1-8.
[15] Y. Zhang, Y. Meng, H. Liu, M. Yang, First-principles study of water desorption from montmorillonite surface, Journal of molecular modeling 22(5) (2016) 105.
[16] Y. Nakatani, N. Ribeiro, S. Streiff, M. Gotoh, G. Pozzi, L. Desaubry, A. Milon, Search for the most 'primitive' membranes and their reinforcers: a review of the polyprenyl phosphates theory, Origins of life and evolution of the biosphere : the

journal of the International Society for the Study of the Origin of Life 44(3) (2014) 197-208.
[17] M. Saco, N. Howe, R. Nathoo, B. Cherpelis, Comparing the efficacies of alginate, foam, hydrocolloid, hydrofiber, and hydrogel dressings in the management of diabetic foot ulcers and venous leg ulcers: a systematic review and meta-analysis examining how to dress for success, Dermatology online journal 22(8) (2016).
[18] E.A. Kamoun, E.S. Kenawy, X. Chen, A review on polymeric hydrogel membranes for wound dressing applications: PVA-based hydrogel dressings, J Adv Res 8(3) (2017) 217-233.
[19] S. Khunmanee, Y. Jeong, H. Park, Crosslinking method of hyaluronic-based hydrogel for biomedical applications, Journal of tissue engineering 8 (2017) 2041731417726464.
[20] S. Hestrin, M. Schramm, Synthesis of cellulose by Acetobacter xylinum. II. Preparation of freeze-dried cells capable of polymerizing glucose to cellulose, The Biochemical journal 58(2) (1954) 345-52.
[21] K.V.S. Hodel, L. Fonseca, I. Santos, J.C. Cerqueira, R.E.D. Santos-Junior, S.B. Nunes, J.D.V. Barbosa, B.A.S. Machado, Evaluation of Different Methods for Cultivating Gluconacetobacter hansenii for Bacterial Cellulose and Montmorillonite Biocomposite Production: Wound-Dressing Applications, Polymers 12(2) (2020).
[22] M. Ul-Islam, T. Khan, J.K. Park, Nanoreinforced bacterial cellulose-montmorillonite composites for biomedical applications, Carbohydrate polymers 89(4) (2012) 1189-97.
[23] X.Y. Chen, H.R. Low, X.Y. Loi, L. Merel, M.A. Mohd Cairul Iqbal, Fabrication and evaluation of bacterial nanocellulose/poly(acrylic acid)/graphene oxide composite hydrogel: Characterizations and biocompatibility studies for wound dressing, J Biomed Mater Res B Appl Biomater 107(6) (2019) 2140-2151.
[24] M.F. Akhtar, M. Hanif, N.M. Ranjha, Methods of synthesis of hydrogels ... A review, Saudi Pharm J 24(5) (2016) 554-559.
[25] W. Treesuppharat, P. Rojanapanthu, C. Siangsanoh, H. Manuspiya, S. Ummartyotin, Synthesis and characterization of bacterial cellulose and gelatin-based hydrogel composites for drug-delivery systems, Biotechnol Rep (Amst) 15 (2017) 84-91.

[26] A. Kasuya, J. Sakabe, Y. Tokura, Potential application of in vivo imaging of impaired lymphatic duct to evaluate the severity of pressure ulcer in mouse model, Sci Rep 4 (2014) 4173.
[27] W. Fang, G. Wang, L. Tang, H. Su, H. Chen, W. Liao, J. Xu, Hydrogen gas inhalation protects against cutaneous ischaemia/reperfusion injury in a mouse model of pressure ulcer, J Cell Mol Med 22(9) (2018) 4243-4252.
[28] J. Liu, E.G. Rybakina, E.A. Korneva, M. Noda, Effects of Derinat on ischemia-reperfusion-induced pressure ulcer mouse model, J Pharmacol Sci 138(2) (2018) 123-130.
[29] A.L. Strong, A.C. Bowles, C.P. MacCrimmon, S.J. Lee, T.P. Frazier, A.J. Katz, B. Gawronska-Kozak, B.A. Bunnell, J.M. Gimble, Characterization of a Murine Pressure Ulcer Model to Assess Efficacy of Adipose-derived Stromal Cells, Plastic and reconstructive surgery. Global open 3(3) (2015) e334.
[30] I. Stadler, R.Y. Zhang, P. Oskoui, M.S. Whittaker, R.J. Lanzafame, Development of a simple, noninvasive, clinically relevant model of pressure ulcers in the mouse, Journal of investigative surgery : the official journal of the Academy of Surgical Research 17(4) (2004) 221-7.
[31] D.J. Langford, A.L. Bailey, M.L. Chanda, S.E. Clarke, T.E. Drummond, S. Echols, S. Glick, J. Ingrao, T. Klassen-Ross, M.L. Lacroix-Fralish, L. Matsumiya, R.E. Sorge, S.G. Sotocinal, J.M. Tabaka, D. Wong, A.M. van den Maagdenberg, M.D. Ferrari, K.D. Craig, J.S. Mogil, Coding of facial expressions of pain in the laboratory mouse, Nature methods 7(6) (2010) 447-9.
[32] F.A. Felipetti, R.M. Bereta, S.M.S. Piedade, P.D. Novaes, Oral Administrations of Hancornia speciosa Gomes Latex Do Not Increase Bone Neoformation, Revista brasileira de ortopedia 54(6) (2019) 692-696.
[33] R. Brandes, L. de Souza, V. Vargas, E. Oliveira, A. Mikowski, C. Carminatti, H. Al-Qureshi, D. Recouvreux, Preparation and characterization of bacterial cellulose/TiO2 hydrogel nanocomposite, J Nano Res 43 (2016) 73-80.
[34] C. Molina-Ramirez, C. Enciso, M. Torres-Taborda, R. Zuluaga, P. Ganan, O.J. Rojas, C. Castro, Effects of alternative energy sources on bacterial cellulose characteristics produced by Komagataeibacter medellinensis, International journal of biological macromolecules 117 (2018) 735-741.
[35] M.S. Abdel-Aziz, K.S. Abou-El-Sherbini, E.M. Hamzawy, M.H. Amr, S. El-Dafrawy, Green Synthesis of Silver Nano-particles by Macrococcus bovicus and Its

Immobilization onto Montmorillonite Clay for Antimicrobial Functionality, Applied biochemistry and biotechnology 176(8) (2015) 2225-41.
[36] R. Velmurugan, T.P. Mohan, Epoxy-Clay Nanocomposites and Hybrids: Synthesis and Characterization, J Reinf Plast Compos 28(1) (2009) 17-37.
[37] M. Ul-Islam, M.W. Ullah, S. Khan, J.K. Park, Production of bacterial cellulose from alternative cheap and waste resources: A step for cost reduction with positive environmental aspects, Korean J Chem Eng 37 (2020) 925–937.
[38] M. Ul-Islam, W.A. Khattak, M.W. Ullah, S. Khan, J.K. Park, Synthesis of regenerated bacterial cellulose-zinc oxide nanocomposite films for biomedical applications, Cellulose 21 (2014) 433–447.
[39] Y. Xu, X. Liu, Q. Jiang, D. Yu, Y. Xu, B. Wang, W. Xia, Development and properties of bacterial cellulose, curcumin, and chitosan composite biodegradable films for active packaging materials, Carbohydrate polymers 260 (2021) 117778.
[40] A. Picolotto, D. Pergher, G.P. Pereira, K.G. Machado, H. da Silva Barud, M. Roesch-Ely, M.H. Gonzalez, L. Tasso, J.G. Figueiredo, S. Moura, Bacterial cellulose membrane associated with red propolis as phytomodulator: Improved healing effects in experimental models of diabetes mellitus, Biomedicine & pharmacotherapy = Biomedecine & pharmacotherapie 112 (2019) 108640.
[41] L.J. Del Valle, A. Diaz, J. Puiggali, Hydrogels for Biomedical Applications: Cellulose, Chitosan, and Protein/Peptide Derivatives, Gels 3(3) (2017).
[42] M. Sirousazar, A. Jahani-Javanmardi, F. Kheiri, Z.M. Hassan, In vitro and in vivo assays on egg white/polyvinyl alcohol/clay nanocomposite hydrogel wound dressings, Journal of biomaterials science. Polymer edition 27(16) (2016) 1569-83.
[43] W.K. Czaja, D.J. Young, M. Kawecki, R.M. Brown, Jr., The future prospects of microbial cellulose in biomedical applications, Biomacromolecules 8(1) (2007) 1-12.
[44] A. Sannino, S. Pappada, M. Madaghiele, A. Maffezzoli, L. Ambrosio, L. Nicolais, Crosslinking of cellulose derivatives and hyaluronic acid with water-soluble carbodiimide, Polymer 46(25) (2005) 11206-11212.
[45] A. Agarwal, J.F. McAnulty, M.J. Schurr, C.J. Murphy, N.L. Abbott, 8 - Polymeric materials for chronic wound and burn dressings, Advanced Wound Repair Therapies 20 (2011) 186-208.
[46] L.G. Ovington, Advances in wound dressings, Clinics in dermatology 25(1) (2007) 33-8.

[47] S.D. Dutta, D.K. Patel, K.T. Lim, Functional cellulose-based hydrogels as extracellular matrices for tissue engineering, Journal of biological engineering 13 (2019) 55.
[48] J.S. Mervis, T.J. Phillips, Pressure ulcers: Pathophysiology, epidemiology, risk factors, and presentation, J Am Acad Dermatol 81(4) (2019) 881-890.
[49] C.B. Nielson, N.C. Duethman, J.M. Howard, M. Moncure, J.G. Wood, Burns: Pathophysiology of Systemic Complications and Current Management, J Burn Care Res 38(1) (2017) e469-e481.
[50] A. Shpichka, D. Butnaru, E.A. Bezrukov, R.B. Sukhanov, A. Atala, V. Burdukovskii, Y. Zhang, P. Timashev, Skin tissue regeneration for burn injury, Stem Cell Res Ther 10(1) (2019) 94.
[51] L. Kvasz, Kuhn's Structure of Scientific Revolutions between sociology and epistemology, Stud Hist Philos Sci 46 (2014) 78-84.
[52] V. Kinte, T. Arabatzis, Kuhn's The structure of scientific revolutions revisited, Routledge, New York, 2012.
[53] T.S. Kuhn, I. Hacking, The structure of scientific revolutions, Fourth edition. ed., The University of Chicago Press, Chicago ; London, 2012.
[54] R. Xu, H. Xia, W. He, Z. Li, J. Zhao, B. Liu, Y. Wang, Q. Lei, Y. Kong, Y. Bai, Z. Yao, R. Yan, H. Li, R. Zhan, S. Yang, G. Luo, J. Wu, Controlled water vapor transmission rate promotes wound-healing via wound re-epithelialization and contraction enhancement, Scientific reports 6 (2016) 24596.
[55] E.Y.X. Loh, N. Mohamad, M.B. Fauzi, M.H. Ng, S.F. Ng, M.C.I. Mohd Amin, Development of a bacterial cellulose-based hydrogel cell carrier containing keratinocytes and fibroblasts for full-thickness wound healing, Scientific reports 8(1) (2018) 2875.
[56] M.H. Kwak, J.E. Kim, J. Go, E.K. Koh, S.H. Song, H.J. Son, H.S. Kim, Y.H. Yun, Y.J. Jung, D.Y. Hwang, Bacterial cellulose membrane produced by Acetobacter sp. A10 for burn wound dressing applications, Carbohydrate polymers 122 (2015) 387-98.
[57] T.G. Sahana, P.D. Rekha, Biopolymers: Applications in wound healing and skin tissue engineering, Molecular biology reports 45(6) (2018) 2857-2867.
[58] P.H. Wang, B.S. Huang, H.C. Horng, C.C. Yeh, Y.J. Chen, Wound healing, Journal of the Chinese Medical Association : JCMA 81(2) (2018) 94-101.

[59] P. Brassolatti, H.W. Kido, P.S. Bossini, P.R. Gabbai-Armelin, A.N. Otterco, L. Almeida-Lopes, L.M. Zanardi, M.A. Napolitano, L. de Avo, L.A. Forato, F.M. Araujo-Moreira, N.A. Parizotto, Bacterial cellulose membrane used as biological dressings on third-degree burns in rats, Bio-medical materials and engineering 29(1) (2018) 29-42.
[60] K.E. Bourakadi, N. Merghoub, M. Fardioui, M.E.M. Mekhzoum, I.M. Kadmiri, E.M. Essassi, A.K. Qaiss, R. Bouhfid, Chitosan/polyvinyl alcohol/thiabendazoluim-montmorillonite bio-nanocomposite films: Mechanical, morphological and antimicrobial properties, Composites Part B: Engineering 172(1) (2019) 103-110.
[61] F. Garcia-Villen, A. Faccendini, C. Aguzzi, P. Cerezo, M.C. Bonferoni, S. Rossi, P. Grisoli, M. Ruggeri, F. Ferrari, G. Sandri, C. Viseras, Montmorillonite-norfloxacin nanocomposite intended for healing of infected wounds, International journal of nanomedicine 14 (2019) 5051-5060.

APÊNDICE A – Figure legends

Fig. 1. FTIR analysis of BC and BC+MMT membrane showing the presence of peaks for different chemical groups.

Fig. 2. Illustration scheme of structure and possible interaction between MMT and BCH.

Fig. 3. SEM analysis of BC and BC+MMT membranes. (A, C) The typical homogeneous tridimensional network of nano and microfibrils of BC surface. (B, D) Microparticles of MMT presented disperse uniformly throughout the BC surface. (E, F) Gross observation of BC membranes without MMT and with MMT, respectively.

Fig. 4. Stress strain curves of BC (black line), and BC+MMT (blue line) composites.

Fig. 5. Effect of BCH-MMT on wound healing and inflammatory signs using the pressure injury model in mice. (A) Wound area (cm^2), (B) wound contraction, (C) exudate, (D) redness, (E) moisture, (F) pain. Data are expressed as mean ± standard error of the mean. Statistical analysis was performed using two-way ANOVA followed by Bonferroni's post-hoc test. *p<0.05, **p<0.01, ***p<0.001 *vs.* control.

Fig. 6. Representative photomicrography of wound healing in the control, Dersani®, and BCH-MMT groups during the course of treatment. Cross-section. CL, clot; EP, epithelium; NE, necrosis; GT, granulation tissue; *, interstitial fluid (edema); **, clot surface (hematoxylin and eosin, 400x).

Fig. 7. Representative photomicrography of the wound healing in the control, Dersani® and BCH-MMT groups. Cross-section. → thin collagenous fibers, *, thick and resistant collagen fibers. (Mallory's trichrome, 400x).

Fig. 8. Effect of BCH-MMT on the number of inflammatory cells using the pressure injury model in mice. Data are expressed as mean ± standard error of the mean. Statistical analysis was performed using two-way ANOVA test followed by Bonferroni's post-hoc test. *p<0.05, **p<0.01, ***p<0.001 *vs.* Control.

APÊNDICE B – Figures

Figure 1

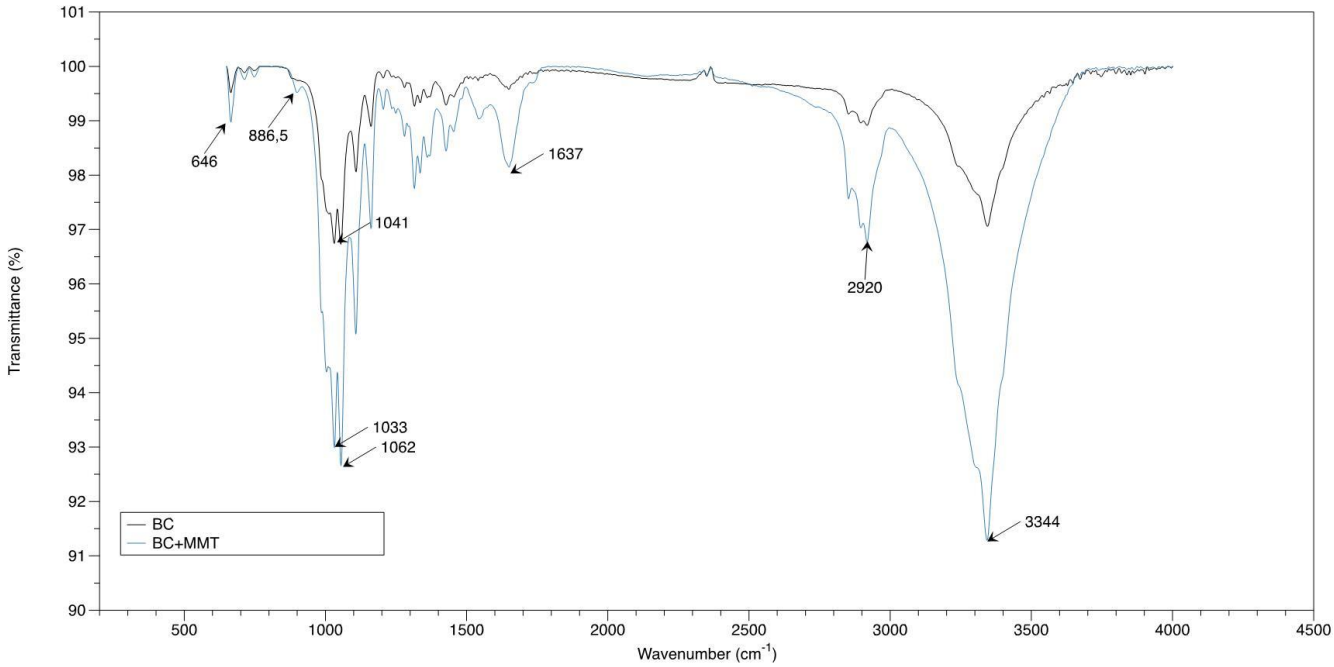

Figure 2

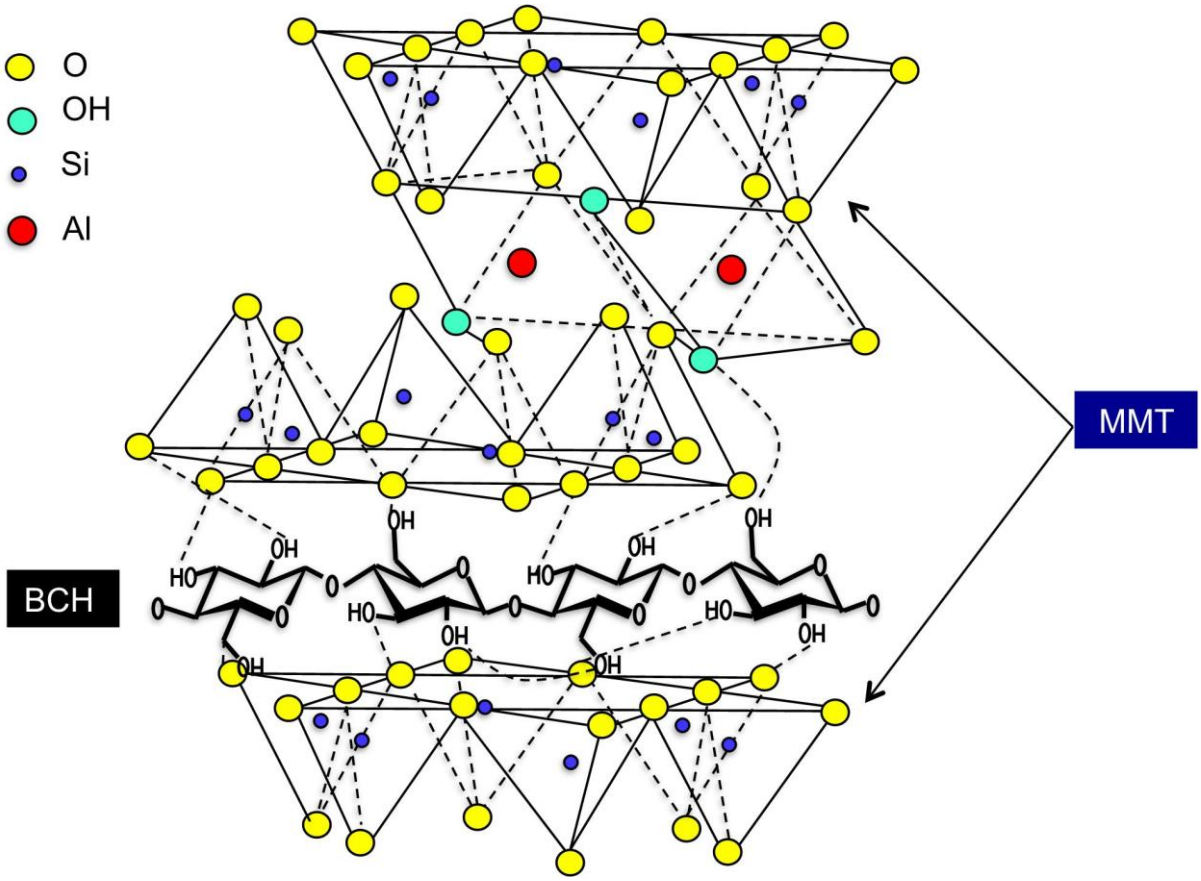

Figure 3

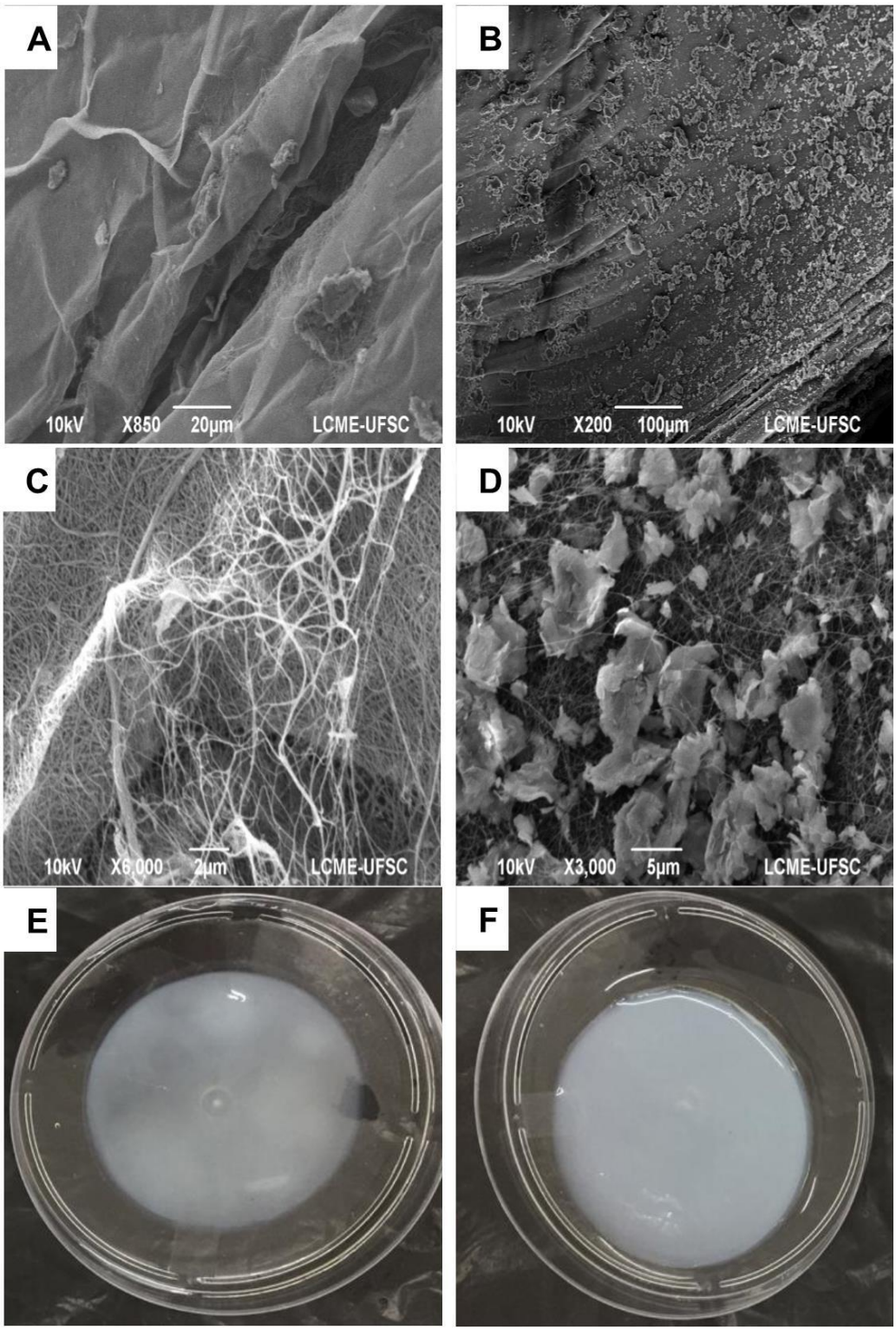
A
10kV X850 20µm LCME-UFSC
B
10kV X200 100µm LCME-UFSC
C
10kV X6,000 2µm LCME-UFSC
D
10kV X3,000 5µm LCME-UFSC
E
F

Figure 4

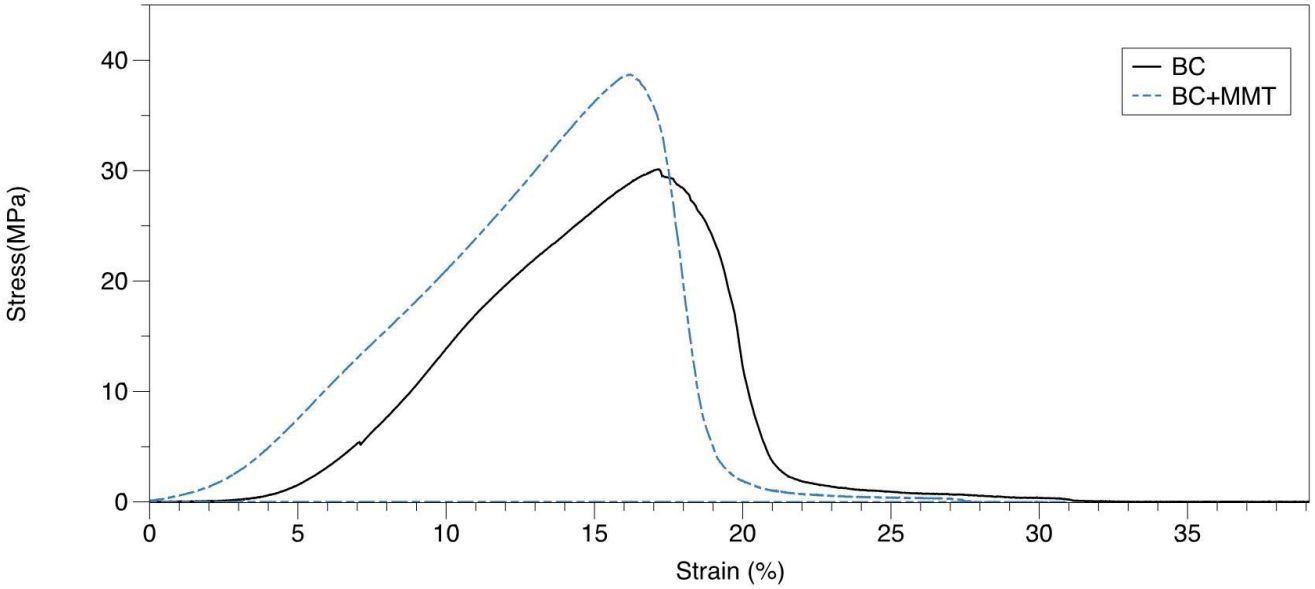

Figure 5

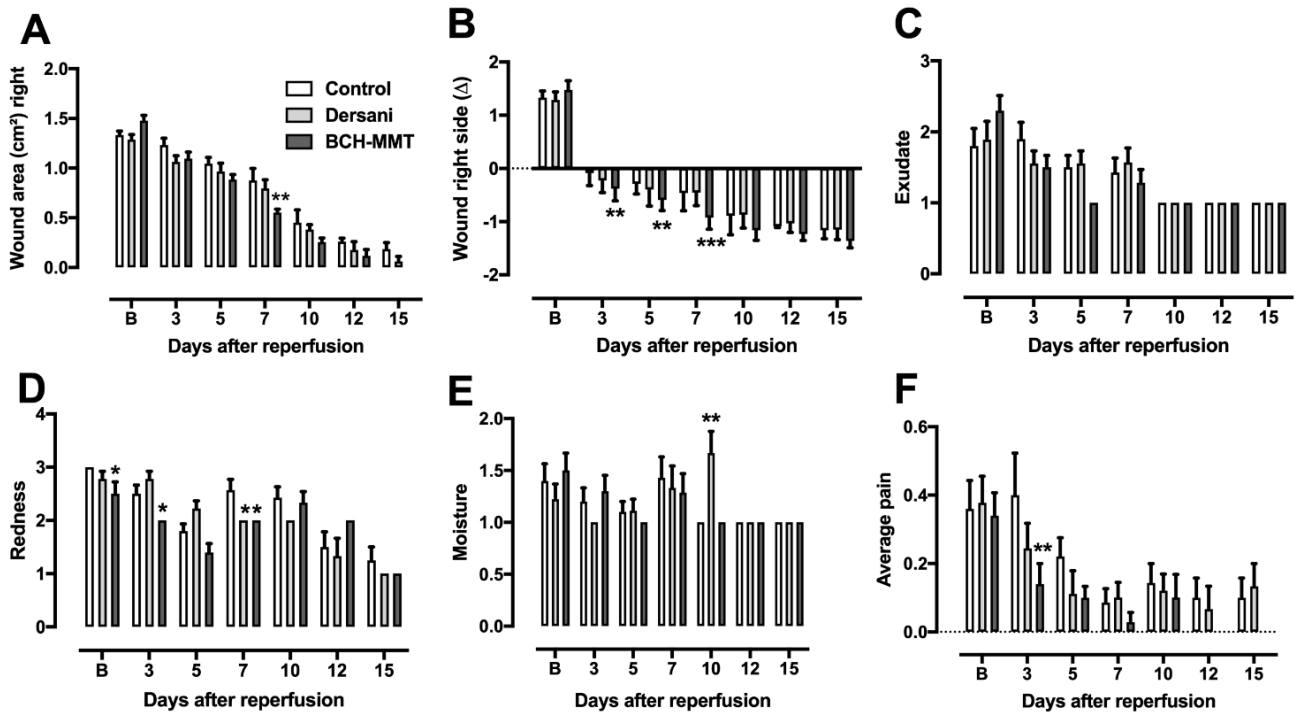
A
Wound area (cm²) right
Control
Dersani
BCH-MMT
Days after reperfusion
B
Wound right side (Δ)
Days after reperfusion
C
Exudate
Days after reperfusion
D
Redness
Days after reperfusion
E
Moisture
Days after reperfusion
F
Average pain
Days after reperfusion

Figure 6

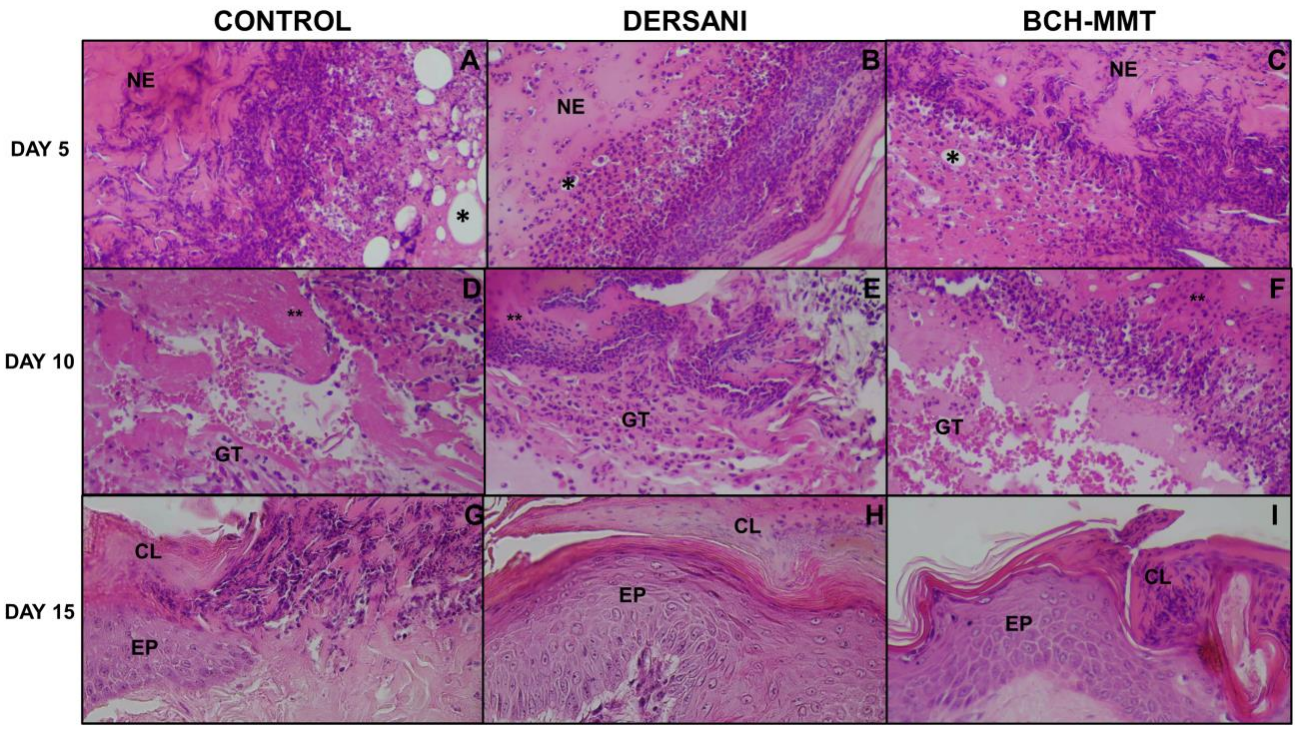
CONTROL
DERSANI
BCH-MMT
DAY 5
DAY 10
DAY 15
A
B
C
D
E
F
G
H
I
NE
*
**
GT
CL
EP

Figure 7

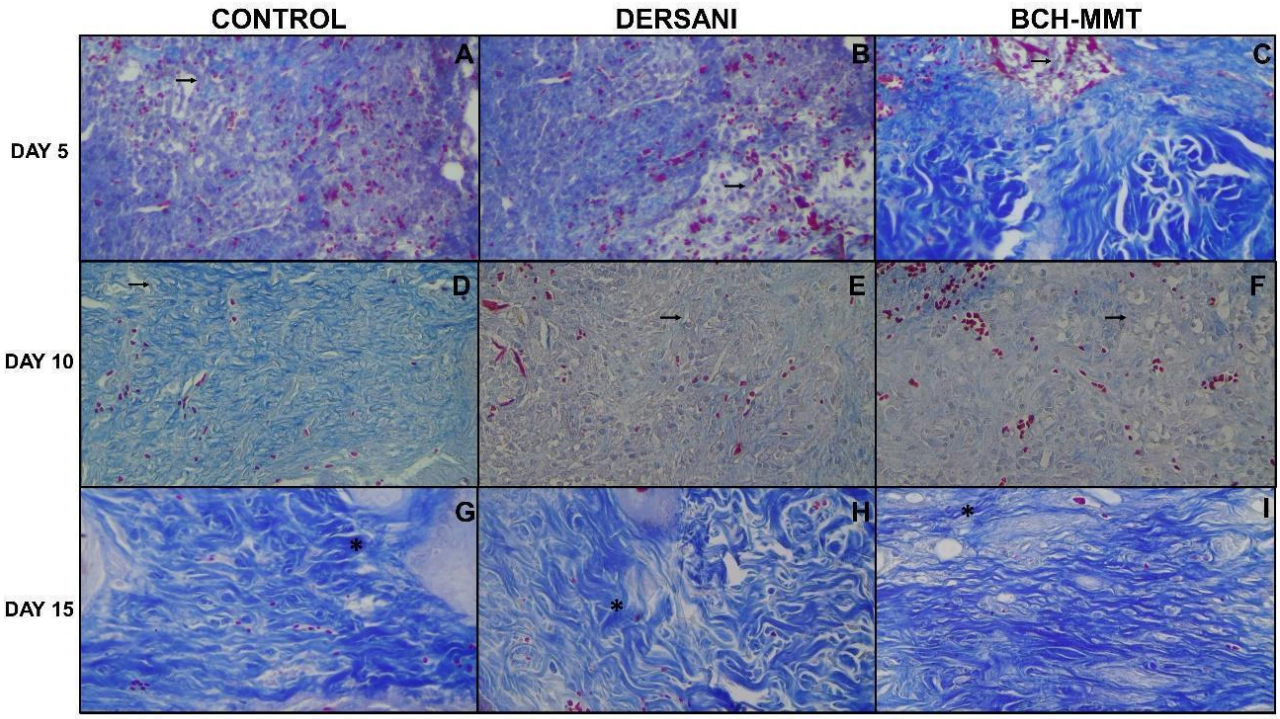

Figure 8

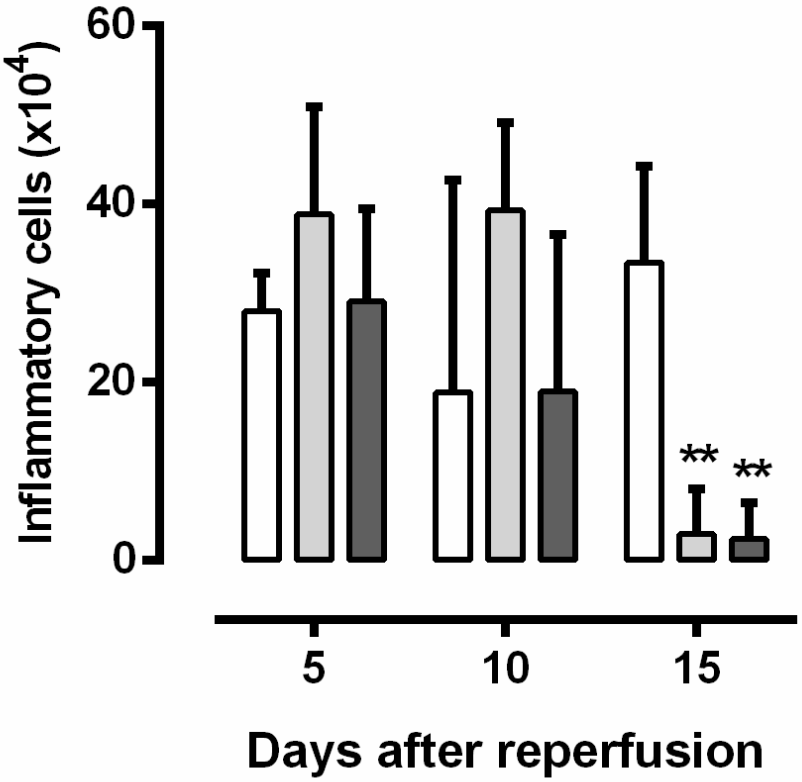
60
40
20
0
Inflammatory cells (x10^4)
**
**
5
10
15
Days after reperfusion

Anexo A - Normas da Revista

International Journal of Biological Macromolecules (Fator de impacto=6.953): https://www.journals.elsevier.com/international-journal-of-biological-macromolecules/editorial-board

Guide for authors: https://www.elsevier.com/journals/international-journal-of-biological-macromolecules/0141-8130/guide-for-authors